Effects of plasma excitation power, sample bias, and duty cycle on the structure and surface properties of amorphous carbon thin films fabricated on AISI440 steel by plasma immersion ion implantation

Z. M. Zeng,[a] X. B. Tian,[a] T. K. Kwok, B. Y. Tang,[a] M. K. Fung, and P. K. Chu[b]
Department of Physics and Materials Science, City University of Hong Kong, Kowloon, Hong Kong

(Received 14 December 1999; accepted 17 March 2000)

Plasma immersion ion implantation is a nonline-of-sight method for fabricating amorphous carbon or diamond-like-carbon coatings on steels to improve the surface properties. In this work, carbon thin films are synthesized on 9Crl8 (AISI440) stainless bearing steel by acetylene (C_2H_2) plasma immersion ion implantation (PIII). The effects of the processing parameters, including rf power, sample voltage pulse duty cycle, and target bias, on the structure and surface properties of the carbon thin films is systematically investigated employing Raman spectroscopy, Auger electron spectroscopy, friction coefficient measurement, and wear test. The results reveal that carbon films several hundred nanometers thick with a well-mixed interface are formed on the 9Crl8 steel after C_2H_2 PIII, but the structure and properties of the carbon films vary greatly under different PIII conditions. There is an optimal process window within which the synthesized films have superior properties, and current densities that are too high do not yield films with the desired performance.
 [S0734-2101(00)00705-3]

I. INTRODUCTION

Diamond-like carbon (DLC) is a desirable material in niche applications due to its superior properties, such as excellent hardness, strong wear resistance, good chemical inertness, high electrical resistivity, as well as unique optical characteristics.[1–4] DLC is a dense, metastable form of amorphous carbon (*a*-C) or hydrogenated amorphous carbon (*c*-C:H) containing a significant sp^3 component.[1,2] There are two basic ways to synthesize a DLC coating. The first method is to decompose a hydrocarbon gas such as methane or ethylene to form *a*-C:H DLC. The second process employs solid carbon sources (vacuum arc source or ion beam sputtering) to deposit nonhydrogenated *a*-C films.[1–4] Several techniques have been developed to deposit DLC coatings, such as sputtering,[5–8] arc ion plating[2,9] cathodic arc,[6,9–11] plasma assisted chemical vapor deposition,[9,11–14] ion beam assisted deposition (IBAD),[3,15] and ion beam deposition.[6,16,17]

Unlike all the above methods, plasma-immersion ion implantation (PIII) is unique in that it combines ion beam assisted deposition with nonline-of-sight operation. It is thus ideally suited for the fabrication of conformal DLC films on nonplanar or complex-shaped industrial components.[4] DLC deposition on silicon and steels by CH_4 and C_2H_2 PIII has been reported.[4,18–22] Carbon ion implantation into steel and amorphous carbon coating deposition on steels by methane plasma immersion ion implantation have also been shown to improve surface properties such as wear, friction, and corrosion.[18,22–25] In this work, we investigate the structure and surface properties of DLC films fabricated on 9Crl8 martensitic stainless steel by C_2H_2 plasmas immersion ion implantation under different process parameters. Our results show that only films produced within a process window possess good properties. The quality of the carbon films is worse (lower sp^3 content) for higher duty cycle and rf power, and it is believed to be due to large local surface heating and excessive collisions from the implanted ions.

II. EXPERIMENT

Industrial grade 9Crl8 steel samples (composition in wt. %: Fe—79.655, Si—0.8, Mn—0.72, P—0.035, S—0.03, C—0.96, and Cr—17.8) in the quenched-and-tempered state were processed. The samples initially received a fine polish to a surface roughness (R_a) of 0.04 μm, followed by an ultrasonic clean in acetone. The PIII experiment was carried out in a multipurpose plasma immersion ion implanter described in details elsewhere.[26] The specimens were mounted on an oil-cooled stage to expedite heat transfer during PIII. However, since heat conduction through the stainless steel specimens was not extremely efficient, some local surface heating on the samples was expected depending on the ion density. The base pressure of the vacuum chamber was 3×10^{-4} Pa. The plasma was generated using 150–500 W 13.56 MHz/rf via an antenna assembly inside the vacuum chamber. Prior to C_2H_2 PIII, the samples were sputter cleaned in an argon plasma for 10 min. Acetylene gas was subsequently introduced into the chamber until the pressure rose to 3×10^{-1} Pa. The plasma was then ignited and C_2H_2 PIII was conducted at a constant pulse width of 30 μs for 2 h. The pulse repetition rate, target bias, and rf power used in the experiments are depicted in Table I. Samples 1–3 were treated using different target bias, samples 3–5 with various pulse repetition, and samples 5–7 using different rf

[a]Also at: Advanced Welding Production & Technology National Key Lab, Harbin Institute of Technology, Harbin, China.
[b]Electronic mail: paul.chu@cityu.edu.hk

TABLE I. Experimental conditions of C_2H_2 PIII.

	Sample No.							
	0 (control sample)	1	2	3	4	5	6	7
Implantation bias voltage (kv)	0	10	20	30	30	30	30	30
Pulse repetition rate (Hz)	0	100	100	100	200	300	300	300
rf power (W)	Untreated	150	150	150	150	150	350	500

power. The implanted ion density and local surface heating increased monotonically from samples 1–7. It should be noted that the duty cycle used in our experiments was not high in the context of PIII even at a repetition rate of 300 Hz. As shown by our results to be discussed later in this article, a high repetition rate is in fact not desirable. The basic amorphous carbon fabrication mechanism was via deposition during the ''off cycles'' of the voltage pulse. During the ''on cycles'' of the voltage pulse, energetic ions were implanted into the surface enhancing ion mixing and thus adhesion of the amorphous carbon films onto the stainless steel substrate. Some sputtering of the deposited materials also occurred during the on cycles depending on the bias voltage.

The chemical structure of the treated 9Crl8 steel samples was determined by Raman spectroscopy. Auger electron spectroscopy was employed to acquire the elemental composition of the surface layer. The coefficient of friction was measured using a ball-on-disk wear tester equipped with a 6 mm diameter silicon nitride ball. The wear tests were conducted using a load of 50 g and a sliding speed of 1.5×10^{-3} m/s. After 5000 cycles, the wear tracks were inspected under an optical microscope and the widths were measured to assess the wear properties.

III. RESULTS AND DISCUSSION

Raman spectroscopy is a common tool to characterize the microstructure of amorphous carbon films. The Raman spectrum acquired from single crystal diamond shows a sharp peak at 1332 cm^{-1}. Two peaks at 1580 cm^{-1} (*G* band) and 1358 cm^{-1} (*D* band) are observed for graphite.[1,18,27,28] Figure 1 displays the Raman spectra of the carbon films fabricated on samples, 1, 3, 5, and 7. For samples 1 and 3, only a broad peak at about 1550 cm^{-1} is visible, and the observation is in line with the results reported by other researchers[27–29] confirming that the films are amorphous. For sample 5, a shoulder becomes visible and the peak around 1550 cm^{-1} shifts upwards. For sample 7, there is another salient peak at about 1370 cm^{-1} and the main peak around 1550 cm^{-1} shifts to about 1580 cm^{-1}, which is the wave number of the main peak of crystalline graphic. Thus, the graphite content in the carbon films increases from sample 1 to 7.

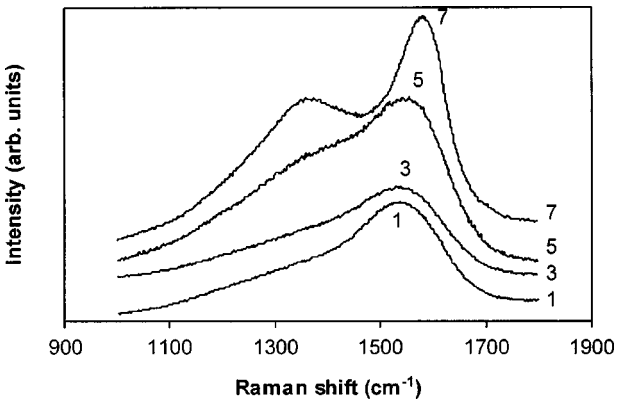

FIG. 1. Raman spectra acquired from samples 1, 3, 5, and 7.

In order to analyze the spectra quantitatively, the Raman spectra are fitted by a least-square program called PEAKFIT. The two deconvoluted peaks are often defined as the disorder (''*D*'') and graphite (''*G*'') peaks. In a high quality DLC film with a high sp^3 content, the *G* peak tends to shift towards a lower frequency and the ratio of the area under the *D* peak to that of under the *G* peak (I_D/I_G) decreases. Figure 2 shows the Raman spectrum of the carbon film on sample 1 and the fitted *G* and *D* profiles are centered at 1545.7 and 1377 cm^{-1}, respectively. Though not shown here, the Raman spectra acquired from the other samples are also fitted by individual *G* and *D* profiles.

Figure 3 compares the position of the *G* peak and intensity ratio (I_D/I_G) under different target bias, pulse repetition rate and rf power. Figure 3(a) shows that the *G* peak position associated with the graphite content (sp^2 to sp^3 ratio) shifts upward with increasing target bias. It indicates that the graphite content (sp^2 bonding fraction) increases and the sp^3 fraction decreases when a higher target bias is used. A similar tendency is found for higher pulse repetition rate and rf power as shown in Figs. 3(b) and 3(c). For sample 7 treated with the highest target bias, pulse repetition rate, and rf power, the wave number of the *G* peak shifts to 1581.9 cm^{-1}, implying that the carbon film formed on sample 7

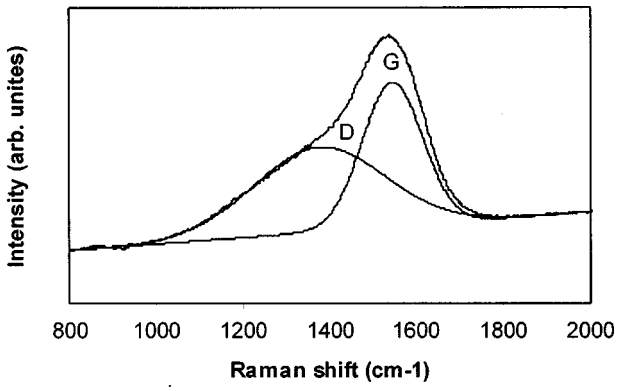

FIG. 2. Raman spectrum of the carbon film deposited on sample 1 by C_2H_2 PIII at 10 kV bias voltage, 100 Hz pulsing rate, and 150 W rf power. The spectrum is fitted by a *G* profile centered at 1545 cm^{-1} and a *D* profile at 1377 cm^{-1}.

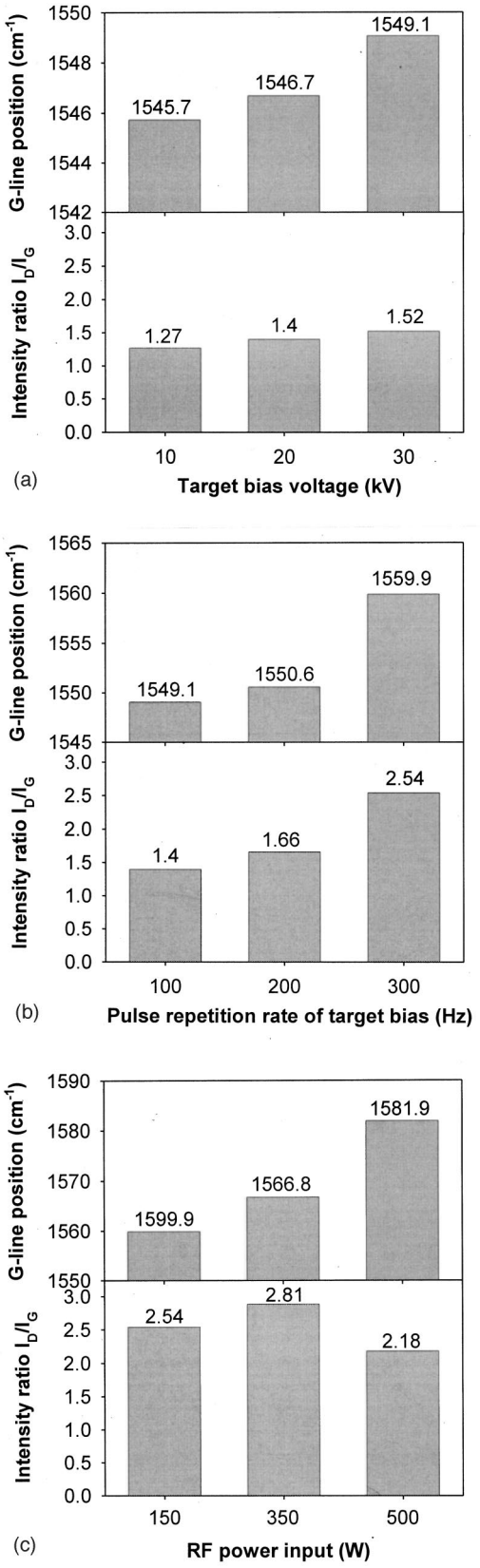

FIG. 3. Raman *G*-peak position and intensity ratio (I_D/I_G) as a function of: (a) target bias voltage, (b) pulse repetition rate, and (c) rf power.

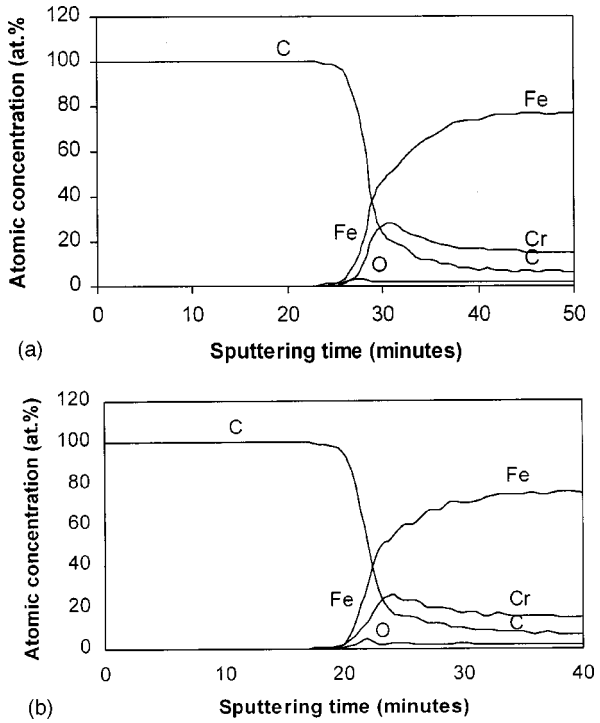

FIG. 4. Auger elemental depth profiles of: (a) sample 2 and (b) sample 5.

contains a very large fraction of graphite. The general observation here is that an ion current density or ion dose that is too high does not yield films with good structure. Even though the samples are cooled, heat conduction from the sample surface to the cooled sample platen is not very efficient and local surface heating is expected when the ion current density is high. The integrity of the amorphous carbon film is degraded due to the development of a short range graphitic structure by thermal effects induced by ion irradiation and the disintegration of the long range structure by atomic collisions when the implant dose is high.[22] Our observation is consistent with the results of DLC films deposited by conventional IBAD.[3]

Figures 4(a) and 4(b) depict the elemental depth profiles acquired from samples 2 and 5 by Auger electron spectroscopy. The average sputtering rate was about 30 nm/min based on crater depth measurements. However, since the carbon film and stainless steel have different sputtering rates, the profiles are shown here on a sputtering time scale to avoid ''overinterpretation'' of the film thickness. A carbon film about 750 nm thick is formed on sample 2. Moreover, carbon atoms have penetrated into the substrate and an approximately 200 nm thick interfacial region in which carbon and substrate elements have been well mixed can be observed. The well-mixed interfacial layer results from favorable ion mixing due to the implanted ions. The thickness of carbon films is about 600 nm in sample 5 and smaller than that of sample 2. As aforementioned, the thickness of the two amorphous carbon films is expected to be similar because of the same processing time. We believe that the discrepancy

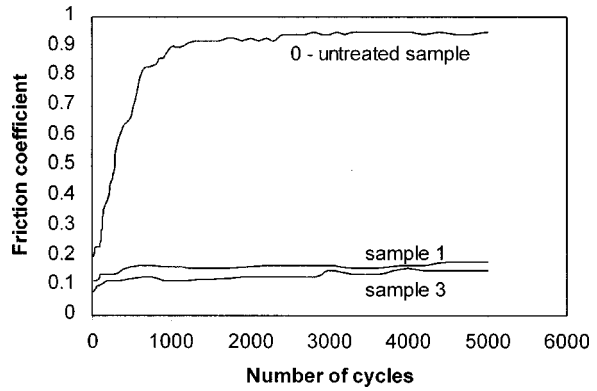

FIG. 5. Coefficient of friction vs number of cycles for samples 0 (untreated), 1, and 3.

revealed by our Auger results stems from the higher sputtering loss due to the more energetic ions and higher ion density and dose as a result of the larger pulse repetition rate.

Figure 5 plots the friction coefficients as a function of the rotating cycles. The friction coefficient of the control sample reaches a relatively high value of 0.8–1.0 quickly. On the contrary, the friction coefficient of the treated sample (samples 1 and 3) remains at a low value (0.1–0.2) throughout the test. Although not shown here, the other treated samples have almost the same friction coefficient values (0.1–0.2) as that of samples 1 and 3. Figure 6 displays the wear track width of each sample after wear tested for 5000 cycles. It is observed that samples 1 to 5 have lower track widths than the untreated sample (sample 0). Among the five samples, samples 2 and 3 have much better wear resistance. In contrast, samples 6 and 7 have larger wear track widths than the untreated sample. Comparing to the Raman results, the inferior wear property can be attributed to the relatively high graphite or sp^2 content in these two films. Therefore, the ion dose rate and implant dose must be controlled carefully in order to fabricate films possessing superior properties. Based on the results acquired from our instrument, there is an optimal process window with respect to the sample bias, pulsing rate and rf power to produce good quality films. Under optimal conditions, there is sufficient ion mixing to enhance the adhesion of the carbon film onto the stainless steel substrate while the heat deposited is insufficient to induce the development of a short range graphite structure and the ion dose is small enough not to create excessive collisions causing substantial conversion from sp^3 to sp^2.

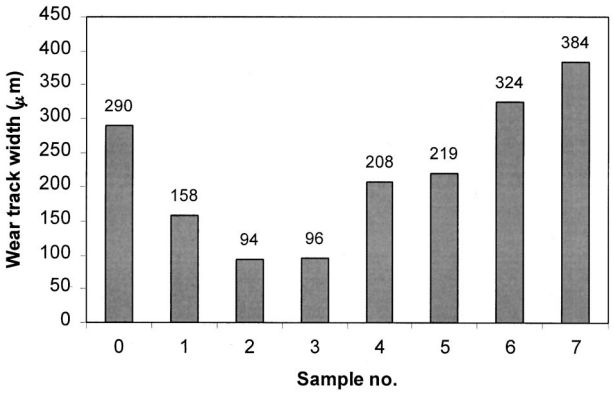

FIG. 6. Comparison of the measured wear track widths of the control (sample 0) and the 7 PIII treated samples.

IV. CONCLUSION

We have investigated the effects of the sample bias, pulsing rate, rf power on the structure and surface properties of amorphous carbon films fabricated on AISI440 steel samples using plasma immersion ion implantation. Films possessing superior properties are produced within a specific process window with respect to the sample bias, pulsing rate, and rf power. Pulsing rates and rf power that are too high increase the sp^2 content in the films and give rise to worse tribological characteristics. Even though ion mixing is beneficial, a high ion current density and dose induce excessive atomic collisions and local surface heating thereby degrading the structure and properties of the amorphous carbon films.

ACKNOWLEDGMENTS

The work was supported by Hong Kong Research Grants Council Earmarked Grant Nos. 9040344 and 9040412 and RGC Germany Joint Schemes 9050084 and 9050150.

[1]S. Zhang, B. Wang, and J. Y. Tang, Surf. Eng. **13**, 303 (1997).
[2]Y. Taki and O. Takai, Thin Solid Films **36**, 45 (1998).
[3]K. Baba and R. Hatada, Nucl. Instrum. Methods Phys. Res. B **121**, 129 (1997).
[4]X. M. He, J. F. Bardeau, D. H. Lee, K. C. Walter, M. Tuszewski, and M. Nastasi, J. Vac. Sci. Technol. B **17**, 822 (1999).
[5]B. Wei and K. Komovopoulos, J. Tribol. **119**, 823 (1997).
[6]Jens Ullmann, Nucl. Instrum. Methods Phys. Res. B **127/128**, 910 (1997).
[7]N. H. Cho, K. M. Krishnan, D. K. Veirs, M. D. Rubin, C. B. Hopper, B. Bhushan, and D. B. Bogy, J. Mater. Res. **5**, 2543 (1990).
[8]J. C. Lascovich, R. Giorgi, and S. Scaglione, Appl. Surf. Sci. **47**, 17 (1991).
[9]E. Liu, B. Blanpain, X. Shi, J. P. Celis, H. S. Tan, B. K. Tay, L. K. Cheah, and J. R. Roos, Surf. Coat. Technol. **106**, 72 (1998).
[10]H. J. Scheibe, B. Schultrich, H. Ziegele, and P. Siemroth, IEEE Trans. Plasma Sci. **25**, 685 (1997).
[11]B. S. Xu, D. Flynn, B. K. Tay, S. Prawer, K. W. Nugent, S. R. P. Silva, Y. Lifshitz, and W. I. Milne, Philos. Mag. B **76**, 351 (1997).
[12]S. R. P. Silva, A. Kapoor, and G. A. J. Amaratunga, Surf. Coat. Technol. **73**, 132 (1995).
[13]M. A. Tamor and W. C. Vassell, J. Appl. Phys. **76**, 3823 (1994).
[14]N. Fourches and G. Turban, Thin Solid Films **240**, 28 (1994).
[15]X. He, W. Li, H. Li, and Y. Fan, Nucl. Instrum. Methods Phys. Res. B **82**, 528 (1993).
[16]Y. P. Guo, K. L. Lam, K. M. Lui, R. W. M. Kwok, and K. C. Hui, J. Mater. Res. **13**, 2315 (1998).
[17]V. Palshin, E. I. Meletis, S. Ves, and S. Logothetidis, Thin Solid Films **270**, 165 (1995).
[18]J. Chen, J. R. Conrad, and R. A. Dodd, J. Mater. Eng. Perform. **2**, 839 (1993).
[19]D. H. Lee, K. C. Walter, and M. Nastasi, J. Vac. Sci. Technol. B **17**, 818 (1999).
[20]K. Volz, W. Ensinger, W. Reiber, B. Rauschenbach, and B. Stritzker, J. Mater. Res. **13**, 1765 (1998).
[21]A. H. Handi, X. Qiu, G. W. Malaczynski, A. A. Elmoursi, S. Simko, M. C. Militello, M. P. Balogh, B. P. Wood, K. C. Walter, and M. A. Nastasi, Surf. Coat. Technol. **103/104**, 395 (1998).
[22]K. Baba and R. Hatada, Surf. Coat. Technol. **103/104**, 235 (1998).
[23]J. Chen, J. Blanchard, J. R. Conrad, and R. A. Dodd, Surf. Coat. Technol. **53**, 267 (1992).

[24]J. Chen, J. R. Conrad, and R. A. Dodd, J. Mater. Process. Technol. **49**, 115 (1995).
[25]J. Chen, J. R. Conrad, and R. A. Dodd, Mater. Sci. Eng., A **161**, 97 (1993).
[26]P. K. Chu, B. Y. Tang, Y. C. Cheng, and P. K. Ko, Rev. Sci. Instrum. **68**, 1866 (1997).
[27]S. Prawer, K. W. Nugent, and D. N. Jamieson, Diamond Relat. Mater. **7**, 106 (1998).
[28]D. Beeman, J. Silverman, R. Lynds, and M. R. Anderson, Phys. Rev. B **30**, 870 (1984).
[29]P. J. Fallon, V. S. Veerasamy, C. A. Davis, J. Robertson, G. A. J. Amaratunga, W. I. Milne, and J. Koskinen, Phys. Rev. B **48**, 4777 (1993).